An improved cerebral vessel extraction method for MRA images

Hua Zou[*], Wen Zhang and Qian Wang
School of Computer, Wuhan University, Wuhan, China

Abstract. To improve the speed and accuracy of cerebral vessel extraction, a fast and robust method is proposed in this paper. First, volume data are divided into sub-volumes by using octree, and at the same time invalid volume data are eliminated. Second, fuzzy connectedness is introduced to achieve fast cerebral vessel segmentation from 3D MRA Images. The values of gradient and Laplacian transformation are then calculated to improve the accuracy of the distance field. Last, the center of gravity is utilized to refine the initial centerline to make it closer to the actual centerline of the vessel cavity. The experiment demonstrates that the proposed method can effectively improve the speed and precision of centerline extraction.

Keywords: Segmentation, cerebrovascular, fuzzy connectedness, image segmentation, centerline extraction

1. Introduction

Cerebrovascular disease is one of the most common neurological diseases and seriously threatens the life and health of human beings. Over the years, the incidence of cerebrovascular disease has been rising steadily. Currently, the diagnostic methods of cerebrovascular disease can be classified into two categories: intervention-based methods and image-based methods. Intervention-based methods are direct and effective, but often bring great pains to the patients [1, 2]. Image-based methods, combining computer technologies with medical science, could provide more objective and accurate information to doctors and do not bring psychological and physical pains to the patients [3-8].

Existing imaging modes mainly include: DSA (Digital subtraction angiography), CTA (Computed tomography angiography), MRA (magnetic resonance angiography), VU (Vascular ultrasound), etc. Among them, MRA with the advantages of non-invasion, no radiation and significant reduction in the side effects, has got very broad applications in the treatments of cerebrovascular disease. When image-based methods are employed in clinical applications, a good visualization of cerebral vessels could provide doctors with better information for analysis. It is a challenging task to get the structure of cerebral vessels in the field of medical visualization. Because cerebral vessels have the features of small shape, special position and complex topology, it is necessary to extract the centerline of cerebral vessels to describe the structure of cerebral vessels. The centerline extraction is useful to compute the diameter of cerebral vessels and estimate the lesion degree. Thus, the centerline extraction of cerebral vessels for MRA images has far-reaching significance to the clinical applications and the diagnosis of

---

* Address for correspondence: Hua Zou, School of Computer, Wuhan University, 299 Ba Yi Road, Wu Chang District, Wuhan 430072, China. Tel.: +86-2768775717; Fax: +86-2768775833; E-mail: zouhua08@gmail.com.

cerebrovascular disease.

The methods of vessels centerline extraction can be divided into several categories [9]: 1) Manual tracking methods [10]; 2) Hessian-based method [11-13]; 3) stochastic tracking methods [14-16]; 4) multiple hypothesis methods [17]; 5) ridge-based methods [18]; 6) model-based methods [19]; 7) deformable model methods [20-22], 8) centerline-based methods [23-25], and so on. Manual tracking method assigns center points slice by slice and constructs a centerline by connecting all these points [10]. The method has a high precision but it is time consuming. Hessian-based methods are commonly used for automatic features detection in shape space based on second-order intensity variations. Lv proposed a centerline extraction method based on Hessian matrix [12]. The method computes the Hessian matrix for each target-voxel in the distance map and uses the scale space analysis to generate a centerline. Stochastic tracking methods are used for vessels tracking and segmentation based on uncertainty analysis or statistical theory. Cheng proposed an automated delineation method for calcified vessels in mammography by using uncertainty techniques [14]. Florin proposed a method of particle filter for coronaries segmentation by using a region-based statistical mixture on intensity distributions [15]. Multiple hypothesis methods are used for segmentation of vessel structures by tracking multiple hypothetical vessel trajectories simultaneously. Friman proposed a multiple hypothesis template tracking method to extract an accurate vessel centerline by using a mathematical vessel template model. This method can get a fast speed and be combined with other segmentation techniques to form robust hybrid methods. Ridge-based methods deal with vessels as local ridges of the image hyper-surface and exploit both edge and region information [18]. These methods may have bad effects when vessels have many branches. Model-based methods track the vessel networks by using the appearance or geometric models to describe the features of vessels. Zou proposed a model-based algorithm for the automated tracking of vascular networks in 2-D digital subtraction angiograms [19]. Deformable models obtain the boundaries of objects through the external and internal forces to constrain the contour geometry and regularity. Level set methods are most used in deformable models and evolve a contour to fit the object boundary through the zero level of a higher dimension function. Manniesing proposed a cerebral vasculature segmentation method by using the level set to model the vessel boundary and achieve good effects [20]. Centerline-based methods focus on extracting the vessel centerline directly and can be utilized to constrain an accurate segmentation of the contours efficiently. Xu proposed an improved algorithm which combined the geometrical topology information with the intensity distribution information to obtain the centerline [23]. Wette, et al. proposed a corkscrew algorithm to extract the centerline. The major drawback of this algorithm was that the computed border points could not form a smooth surface in 3D or a closed curve in planes perpendicular to the centerline [24].

All the methods above can extract the centerline of vessels, but the low processing speed is the common bottleneck. To solve this problem, a method for extracting vessels centerlines with higher speed and accuracy is proposed in this paper. The method eliminates invalid volume data by using octree, and refines the centerline by using the center of gravity. The experimental result shows that the proposed method can effectively improve the speed and precision of centerline extraction.

2. Materials and methods

To improve the speed and accuracy of cerebral vessel extraction, a fast and robust method is proposed in this paper. First, the volume data are divided into sub-volumes by using octree, and at the
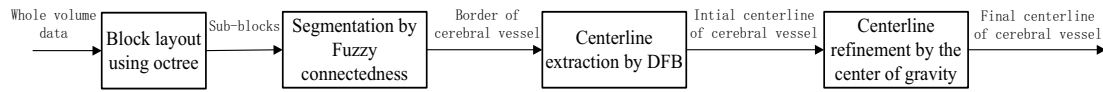
Fig. 1. The flow diagram of the proposed method.

same time invalid volume data are eliminated. Then fuzzy connectedness is introduced to realize fast cerebral extraction from MRA images. The values of gradient and Laplacian transformation are calculated to improve the accuracy of distance field. Last, the center of gravity is used to refine the initial centerline to make it closer to the actual centerline of the vessel cavity. The flow diagram of the process is shown in Figure 1.

2.1. Octree

Octree is a tree-form data structure used to describe three-dimensional space. Each node of octree presents the voxel of a cube and has eight child nodes. The sum of volume corresponding to the children nodes is equal to the volume corresponding to the father node. The octree structure is defined as follows:

Struct Octree
{
char   LevelX, LevelY, LevelZ;   //   depth values of octree in x, y, z directions.
unsigned int X_{min}, X_{max}, Y_{min}, Y_{max}, Z_{min}, Z_{max};   //coordinate range of the octree node in x, y, z directions.
bool   IsLeaf;   //   a bool value
int   Min_value, Max_value;   //   Minimum and maximum values of the octree node
Octree*   Children[8];   // The child nodes of the octree node
}

The depth values of the octree in three directions are assigned first and then the octree is initialized according to the depth values. Root node of the octree presents the whole dataset and its depth value equals to 0. The Root node has eight children nodes whose depth value is 1. The volume data are divided based on the space position layer by layer. On each layer, the volumes corresponding to the octree nodes are subdivided into eight sub-blocks along the orthogonal coordinate axes of the tree. The correlative information is stored in the children nodes of current octree nodes and the depths of children nodes increase by 1. When the depth of the octree node is equal to the pre-set depth, the subdivision is stopped. Each octree node is a leaf node if its depth equals to the specified value. When segmenting cerebral vessels, the minimum and maximum values of each block are compared to the given threshold to determine whether the block should be ignored, so that only sub-blocks including blood vessel voxels are processed.

2.2. Segmentation

In this paper, the fuzzy connectedness method is utilized to extract the boundary of cerebral vessels from MRA images [26]. First, some objective seeds region S_o and background seeds S_1 should be selected in an interactive way before the segmentation procedure by users. Then, for each voxel p in the volume dataset, the fuzzy connectedness of S_b and S_o should be computed respectively, and the relationship of voxel p is calculated according to Eq. (1):

$$R(p) = \mu(p, S_0) / \mu(p, S_0) \tag{1}$$

where $\mu(p, S_0)$ represents the local fuzzy connectedness between p and S_0 in MRA images and $\mu(p, S_1)$ represents the local fuzzy connectedness between p and S_1 in MRA images.

When R > 1, the point p belongs to objective region. When R ≤ 1, the point p belongs to background region. Then, the algorithm can be mainly divided into the following steps:

Step 1: An objective MRA image dataset is chosen, and displayed from three cross sections, which are coronal view, sagittal view and transverse view, respectively, as shown in Figure 2 with grey images;

Step 2: The whole volume data is browsed in the three views slice by slice. Some objective seeds S_0 and some background seeds S_1 are selected by hand;

Step 3: The fuzzy connectedness of the point p *is* calculated, and the relationship whether the point p belongs to the objective region or the background region is determined according to Eq. (1);

Step 4: The segmentation of the cerebral vessels is generated.

If the traversal method is selected for the segmentation procedure to compute the global optimal value of the fuzzy connectedness for each point, a large amount of computation is needed. To improve the efficiency of the algorithm, the dynamic programming method is selected in the segmentation procedure and an adjacent path $m = 6$ for the volume dataset is chosen to compute the fuzzy connectedness.

2.3. Distance from boundary

Distance from Boundary (DFB) is defined as the distance of the target voxel to the nearest boundary. Daniel, et al. [25] calculated the input of DFB as the binary data after segmentation, i.e., the target voxel in the vessel and background. Thus, when DFB is calculated, all the original values of target voxels in the vessels are same which loses the original feature. In this paper, we mark the position of the segmented target voxels, based on which we calculate the gradient and perform Laplacian transformation on the target voxels in the source data. Then, we set the original value of DFB as the sum of gradient inverse and Laplacian transformation. As a result, the closer to the centerline a target voxel is, the bigger of its original value becomes, and vice versa. Therefore, we increase the weighing factor of the target voxels which are closer to the centerline for computing the DFB while decreasing the weighing factor of the target voxels located in the boundary. We use the Euclidean distance to compute DFB. The Euclidean distance between any two adjacent voxels in the space can be expressed by value $1, \sqrt{2}, \sqrt{3}$ based on their relative space position. To simplify the calculation, we use value 10, 14, 17 to replace value $1, \sqrt{2}, \sqrt{3}$ as shown in Figure 2.
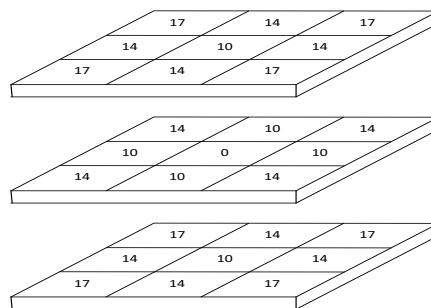

Fig. 2. The Euclidean distance of the point in 3D space.

It is assumed that any point in 3D DFB field has an initial distance value which equals to $f$start(p) and it becomes $f(i, j, k)$ after calculation. $N^3(p)$ denotes the 26 neighborhoods of the point p and can be divided into three categories: $N^{3-1}(p)$, $N^{3-2}(p)$ and $N^{3-3}(p)$. They denote the nearest neighborhood, the diagonal neighborhood in face and the diagonal neighborhood in volume, respectively.

$$f_{start}(p) = 1/fG + fL \tag{2}$$

where f_G is the gradient value of current point, and f_L is the Laplacian transformation value of current point. Utilizing the 26 neighborhoods of the point p, the distance of the three types of neighborhoods can be calculated according to Eq. (3):

$$\begin{aligned} f(N^{3-1}(p)) &= \min(f_{start}(N^{3-1}(p))+10) \\ f(N^{3-2}(p)) &= \min(f_{start}(N^{3-2}(p))+10) \\ f(N^{3-3}(p)) &= \min(f_{start}(N^{3-3}(p))+10) \end{aligned} \tag{3}$$

Finally,

$$f(i,j,k) = \min(f(N^{3-1}(p)), f(N^{3-2}(p)), f(N^{3-3}(p))) \tag{4}$$

Utilizing the octree, calculating DFB can be accelerated by ignoring the invalid sub-blocks which do not contain cerebral vessels.

2.4. Maximum spanning tree

The procedure of building the maximum spanning tree follows the idea of Dijkstra dynamic programming and is implemented as follows [27]: the target voxels in vessels are represented by the nodes of the tree; each non-root node directs to its parent node and a directed tree is generated to link all the voxels in vessels. DFB is utilized to build the maximum spanning tree where the weight from node P_j to P_i is w_{ij} = DFB (P_i), i.e., the cost to link nodes P_j and P_i is w_{ij}.

The procedure of building the maximum spanning tree is described in detail below:

Step 1, Start from the origin P, set the node P as the parent node and make all its 26 neighborhoods direct to P. Add DFB of the 26 neighborhoods to the queue S.

Step 2, Select the node P_{max} with the maximum DFB from S and link the unprocessed nodes in the 26 neighborhoods of C to P_{max}. Set P_{max} as the parent node of these unprocessed nodes and add their DFBs to the queue S.

Step 3, Continue the loop until all the target voxels in vessels are processed.

To improve the efficiency of the procedure, a fast queue sorting method is employed in the procedure: first, a dynamic index table is built whose range is within the interval [0, 255]; then all DFBs of target voxels are normalized in the interval [0, 255] and the corresponding target voxels are added to the table according to their indexes; Finally, target voxels are chosen from the table in the descending order of their indices.

2.5. Path extraction

As the trunk of the maximum spanning tree is the centerline of cerebral vessels, it is only needed to extract the trunk of the maximum spanning tree. If the end point is not specified, the point of the

maximum DFB value defaults to the path terminal E. According to the direction of the node, point E can be directly connected to the source node S.

Although the trunk of the maximum spanning tree can be denoted as the centerline of cerebral vessels, all the points of trunk cannot be ensured to be the centers of gravity which will cause an error of the center path extraction. The center path extraction is corrected with a centroid method which makes the corrected center path stay close to the true center path of vascular as much as possible.

The gravity center of 2D gray image is defined as shown in Eq. (5):

$$C = \min_{x,y}[x_c, y_c] = \left(\frac{\sum_{x,y\in\Omega} xw(x,y)}{\sum_{x,y\in\Omega} w(x,y)}, \frac{\sum_{x,y\in\Omega} yw(x,y)}{\sum_{x,y\in\Omega} w(x,y)} \right) \tag{5}$$

Where B presents the objective region contained in the boundary of cerebral vessels, $w(x, y)$ is the weight and its value equals to $a*(f_{2D}(x, y)-m)$, a is a coefficient of weight, and $f_{2D}(x, y)$ is the value of pixel in the position (x, y) of B [21]. In this paper, $a=-1$, $m= \max_{x,y\in\Omega}(f_{2D}(x,y))$.

Due to small diameter of cerebral vessels, the error of the central path extraction is relatively small. Each point in the centerline is traversed and the normal vector of the point is calculated to determine the cross section. Finally, the center of gravity of the cross sections is calculated, and then is as the point of the corrected centerline.

3. Results and discussion

A head aneurysm dataset is used to verify the rationality and effectiveness of the method proposed in this paper. The dataset is composed of $512 \times 512 \times 512$ voxels with the actual size of 100 mm in *X, Y* and *Z* directions, and stored in 8 bits with a capacity of 128 MB.

The experimental platform is shown as follows: CPU is Intel I5 3.2 GHz, memory is DDR3 4.0 GB, GPU is NVIDIA GeForce GTX650, the size of GPU memory is 1G, and the programming environment is Visual Studio C++.NET 2012.

Octree has significant advantages in efficiently accelerating the process of segmenting vessels voxels and the process of establishing DFB filed. The comparison of the performances between the octree subdivision algorithm and the global traversal algorithm is listed in Table 1. Obviously, the octree method takes less time in the segmentation process and the DFB field establishment than the global traversal algorithm. The experimental result shows that the octree with the block size of 16 ×

Table 1

Experimental datasets

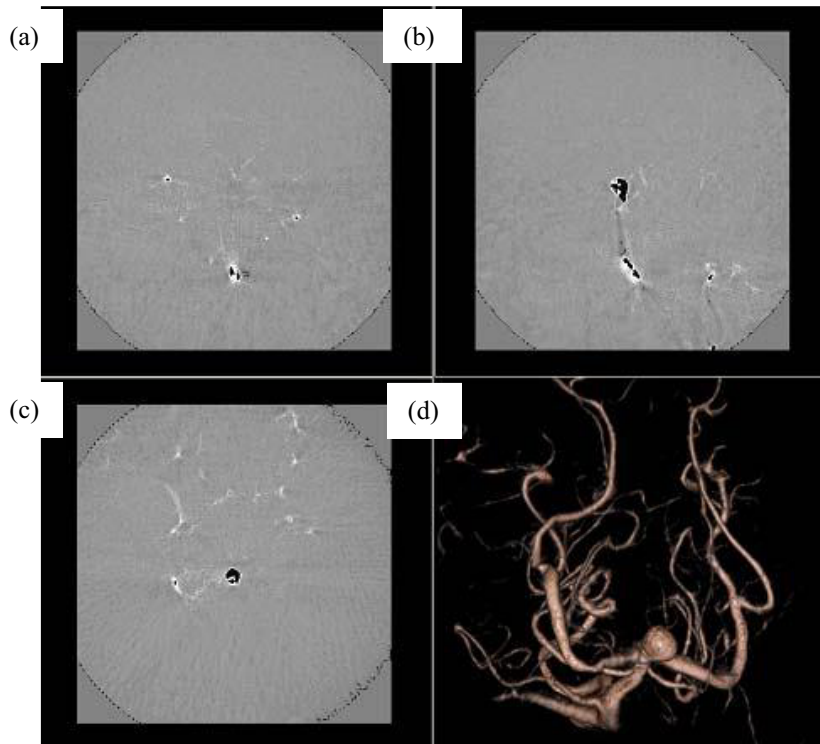| Octree Depth	Octree			Global traverse	
	Octree Construction	Segmentation	DFB Construction	Segmentation	DFB Construction
3	0.08	2.86	3.14	2.86	3.14
4	0.11	2.54	2.84	2.86	3.14
5	0.16	2.10	2.76	2.86	3.14
6	0.21	1.98	2.63	2.86	3.14
7	0.27	1.95	2.52	2.86	3.14
8	0.35	1.94	2.41	2.86	3.14

Fig. 3. Graphical user interface of experimental platform, (a) is coronal view, (b) is sagittal view, (c) is transverse view, (d) is the result of segmentation.

16 × 16 has the best performance, which takes the least time in total and reduces the time by 56.1% compared to the global traversal method. The fuzzy connectedness method is combined with octree in this paper to segment cerebral vessels interactively, and the result is shown in Figure 3.

To verify the accuracy of the proposed method, five types of paths are extracted. Path 1 is an average path of many paths extracted manually, which is considered as the reference path; Path 2 is a path extracted by DFB method [11]; Path 3 is the result of using the 2D cross-sectional analysis method proposed by Kumar [17]; Path 4 is the result of using Hessian Matrix proposed by Lv [12]; and Path 5 is the result of using the method proposed in this paper.

In the experiment, the vessel path named No. 1 is extracted. No. 1 is composed of 50 points as shown in Figure 4(a), while No. 2 is composed of 40 points as shown in Figure 4(b). In both two figures, the blue line denotes the distance between path 2 and the reference path, the red line denotes the distance between path 3 and the reference path, the green line denotes the distance between path 4 and the reference path, the purple line denotes the distance between path 5 and the reference path. The horizontal coordinate of the two figures represents the sequence number of the points in paths, and the vertical coordinate represents the distance between the points in paths and the corresponding points in the reference path, which is measured by voxel.

In Figure 4(a), the average value of the blue lines is 3.792 which means the distance between path 2 and the reference path is 3.792 in voxel; the average value of the red lines is 2.78, the average value of the green lines are 2.576, and the average value of the purple lines are 2.262, which indicates that the centerline of method 4 is closest to the actual. In Figure 4(b), the average value of the blue lines is 3.278, the average value of the red lines is 2.585, the average value of the green lines is 2.49, and the
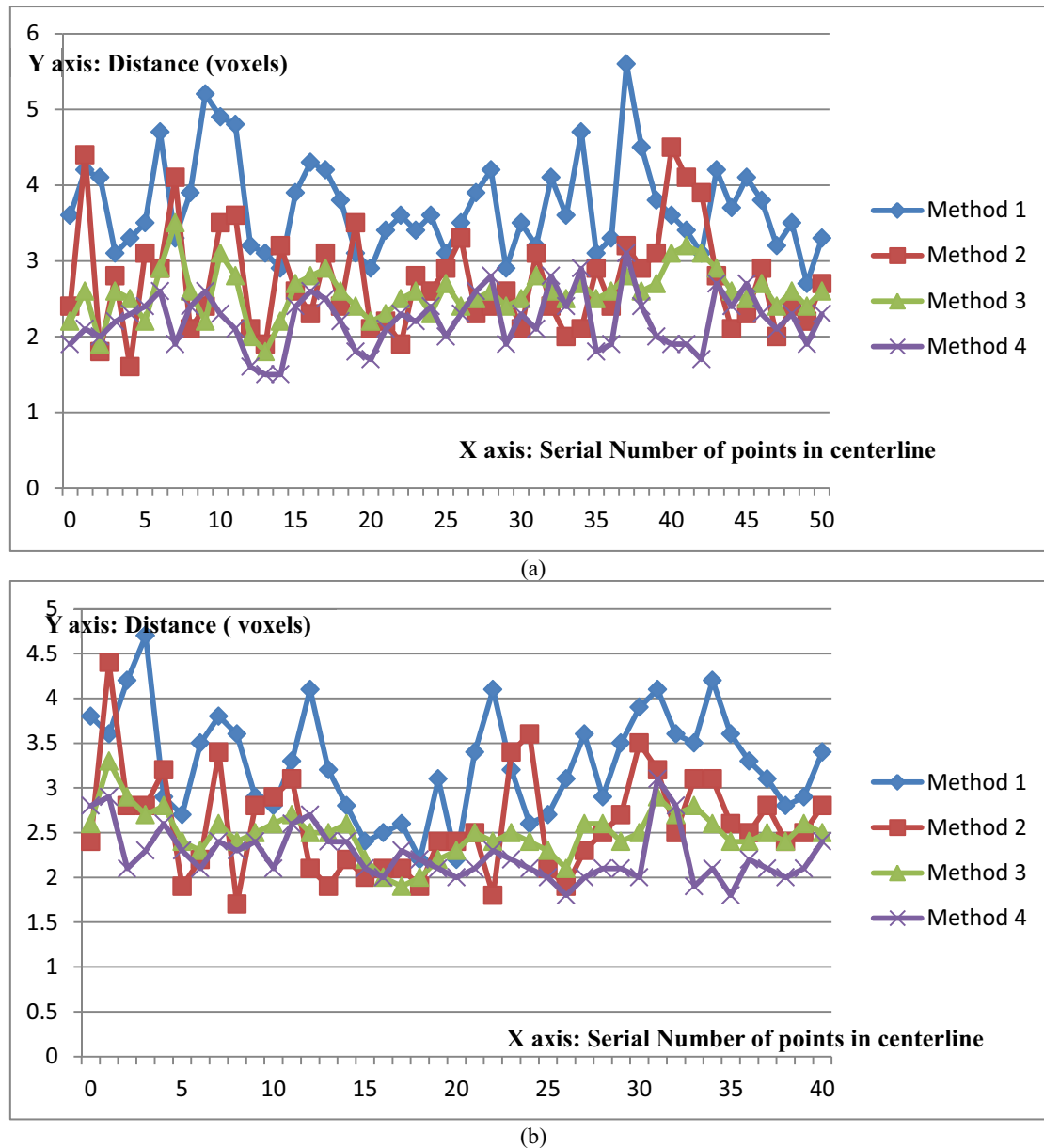
(a)

(b)

Fig. 4. The accuracy comparison between the proposed method and the methods of the same kind. Distances between the centerline of the proposed methods and the centerline assigned by hand are counted. Method 1 is DFB, Method 2 is the 2D cross-sectional analysis method, and Method 3 is the method proposed in this paper. (a) is the No. 1 path, and (b) is the No. 2 path.

In the two above figures, the blue lines are above both the red lines and the green line, which indicates that path 5 is the closest to the reference path. Therefore, the method proposed in this paper can get a better result than method 1, method 2 and method 3. Virtual endoscopy visualization of this vessel aneurysm dataset by using path 4 is shown as Figure 5.
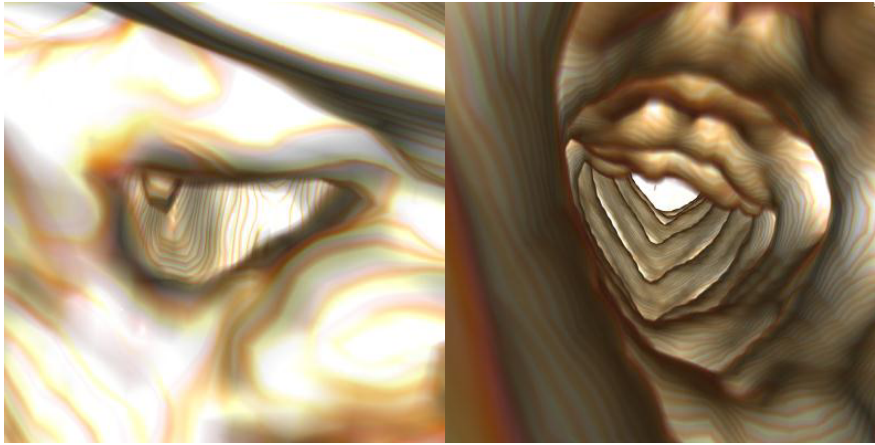
Fig. 5. Virtual endoscopy of the two centerlines extracted by the proposed method.

4. Conclusion

Aiming at extracting the centerline of cerebral vessels with a high precision, a robust and fast extraction method based on octree and fuzzy connectedness is proposed in this paper. First, the volume data are divided into sub-volumes using octree, and invalid volume data are eliminated. Second, fuzzy connectedness is introduced to achieve fast cerebral vessel segmentation from 3D MRA data. The values of gradient and Laplacian transformation are then calculated to improve the accuracy of the distance field. Last, the center of gravity is used to refine the initial centerline to make it closer to the actual centerline of the vessel cavity. The experimental results show that the proposed method can effectively improve the speed and precision of centerline extraction.

Acknowledgment

References

[1] Y. Sun, Automated identification of vessel contours in coronary arteriograms by an adaptive tracking algorithm, IEEE Transactions on Medical Imaging **8** (2006), 78–88.

[2] E.L. Bolson and F.H. Sheehan, Quantification of asynchronous displacement of heart borders, Proceeding of Computers in Cardiology, Chicago, 1990, pp. 613–616.

[3] Z.P. Hang, F.L. Yi, S.Z. Jiang, Z. Jie, et al., The segmentation of liver and vessels in CT images using 3D hierarchical seeded region growing, International Conference on Computer Science and Automation Engineering, Shanghai, 2011, pp. 264–269.

[4] X. Changyan, S. Marius, S. Denis, et al., A strain energy filter for 3D vessel enhancement with application to pulmonary CT images, Medical Image Analysis **15** (2011), 112–124.

[5] R. Florence, B. Maddalena, C. Alexandre, B. Isabelle and P. Michel, A morphological approach for vessel segmentation in eye fundus images with quantitative evaluation, Journal of Medical Imaging and Health Informatics **1** (2011), 42–49.

[6] H.F. Amir, A.Z. Reza, S. Yoshinobu and H. Masatoshi, A hessian-based filter for vascular segmentation of noisy hepatic

CT scans, International Journal of Computer Assisted Radiology and Surgery **7** (2012), 199–205.

[7] D. Klaus, M. Steven, O. Cristina and W. Stefan, A framework for validation of vessel segmentation algorithms, 2013 IEEE 26th International Symposium on Computer-Based Medical Systems, Porto, 2013, pp. 518–519.

[8] D. Klaus, C. Oyarzun and W. Stefan, Interventional planning of liver resections: An overview, Engineering in Medicine and Biology Society (EMBC), San Diego, 2012, pp. 3744–3747.

[9] L. David, A.D. Elsa, B. Isabelle and F.L. Gareth, A review of 3D vessel lumen segmentation techniques: Models, features and extraction schemes, Medical Image Analysis **13** (2009), 819–845.

[10] Y. Ge, D. Stelts, J. Wang and D. Vining, Computing the centerline of the colon: A robust and efficient method based on 3D skeletons, Journal of Computer Assisted Tomography **23** (1999), 786–794.

[11] S.R. Aylward and E. Bullitt, Initialization, noise, singularities, and scale in height ridge traversal for tubular object centerline extraction, IEEE Transactions on Medical Imaging **21** (2002), 61–75.

[12] X.R. Lv and X.B. Gao, Centerline extraction based on hessian matrix and scale space analysis, International Conference on Information Engineering and Computer Science, Wuhan, 2009, pp. 1–4.

[13] J.Z. Cheng, B.C. Elodia, E.D. Pisano and D. Shen, Detection of arterial calcification in mammograms by random walks, Information Processing in Medical Imaging **5636** (2009), 713–724.

[14] J.Z. Cheng, C.M. Chen, E.B. Cole, et al., Automated delineation of calcified vessels in mammography by tracking with uncertainty and graphical linking techniques, IEEE Transactions on Medical Imaging **31** (2012), 2143–2155.

[15] C. Florin, N. Paragios and J. Williams, Particle filters, a quasi-monte carlo solution for segmentation of coronaries, Medical Image Computing and Computer-Assisted Intervention–MICCAI **3749** (2005), 246–253.

[16] Ola Friman, A. Hennemuth, A. Harloff, et al., Probabilistic 4D blood flow tracking and uncertainty estimation, Medical Image Analysis **15** (2011), 720–728.

[17] Ola Friman, M. Hindennach, C. Kuhnel and H.O. Peitgen, Mutiple hypothesis template tracking of small 3D vessel structures, Medical Image Analysis **23** (2010), 160–171.

[18] S. Joes, D. Michael, N. Meindert, et al., Ridge-based vessel segmentation in color images of the retina, IEEE Transactions on Medical Imaging **23** (2004), 501–509.

[19] P. Zou, P. Chan and P. Rockett, A model-based consecutive scanline tracking method for extracting vascular networks from 2-D digital subtraction angiograms, IEEE Transactions on Medical Imaging **28** (2009), 241–249.

[20] B. Hrvoje, P.M. Jose, C.V. Maria, et al., Automated segmentation of cerebral vasculature with aneurysms in 3DRA and TOF-MRA using geodesic active regions: An evaluation study, Medical Physics **38** (2011), 210–222.

[21] R. Manniesing, B.K. Velthuis, M.S. Leeuwen, et al., Level set based cerebral vasculature segmentation and diameter quantification in CT angiography, Medical Image Analysis **10** (2006), 200–214.

[22] R. Manniesing, M.A. Viergever and W.J. Niessen, Vessel axis tracking using topology constrained surface evolution, IEEE Transactions on Medical Imaging **26** (2007), 309–316.

[23] Y. Xu, H. Zhang, H. Li and G.S. Hu, An improved algorithm for vessel centerline tracking in coronary angiograms, Computer Methods and Programs in Biomedicine **88** (2007), 131–143.

[24] P. Wette, S. Arens, A. Elsner and G. Domik, Extending the corkscrew algorithm to find bifurcations of vessels, Proceedings Computer Graphics and Imaging, Innsbruck, 2010, pp. 317–323.

[25] J.B. Daniel and A.R. Richard, Center line algorithm for virtual endoscopy based on chamfer distance transform and Dijkstra's single-source shortest-path algorithm, Medical Imaging 1999: Physiology and Function from Multidimensional Images **3660** (1999), 225–233.

[26] K.U. Jayaram and S. Supun, Fuzzy connectedness and object definition: Theory, algorithms, and applications in image segmentation, Graphical Models and Image Processing **58** (1996), 246–261.

[27] C.J. Alpert, T.C. Hu, J.H. Huangang and A.B. Kahng, Prim-Dijkstra tradeoffs for improved performance-driven routing tree design, IEEE Transactions on Computer-Aided Design of Integrated Circuits and Systems **14** (1995), 890–896.